Virchows Arch (1995) 427:415–421

ORIGINAL ARTICLE

A. Malandrini · T. Cavallaro · G.M. Fabrizi · G. Berti
R. Salvestroni · C. Salvadori · G.C. Guazzi

Ultrastructure and immunoreactivity of dystrophic axons indicate a different pathogenesis of Hallervorden-Spatz disease and infantile neuroaxonal dystrophy

Received: 23 November 1994 / Accepted: 6 June 1995

Abstract An immunohistochemical and ultrastructural analysis of dystrophic axons (DAs) in the brain and peripheral nerve of a patient with familial infantile neuroaxonal dystrophy (INAD) and in the brain of a patient with familial Hallervorden-Spatz Disease (HSD) revealed prevalent membrano-tubular or granulo-vesicular profiles with a graded pattern of evolution in INAD, while dense bodies, vesicles and amorphous material were present in HSD. DAs immunoreactivity with τ-protein and 200 kDa-neurofilament antibodies was stronger in HSD than in INAD. In both cases immunohistochemistry was positive for ubiquitin and negative for β-tubulin and β-amyloid. Distinct ultrastructural features and immunoreactivity pattern of cytoskeletal components suggest different pathogenetic mechanisms.

Key words Hallervorden-Spatz disease · Infantile neuroaxonal dystrophy · Axonal dystrophy · Ultrastructure · Cytoskeletal proteins

Introduction

Neuroaxonal dystrophy (NAD) is a degenerative process of the central and peripheral nervous systems [7, 16, 17]. Morphologically, it is characterized by swollen axons containing different types of structured and/or amorphous material [1, 4, 5, 15, 17]. The pathological process seems to start from the neuritic terminal and proceed back to the perikaryon, suggesting an impairment of retrograde axonal transport [17, 20].

NAD occurs in some areas of the central neurons system (CNS) during normal aging, but also represents the morphological hallmark of early-onset disorders, such as Hallervorden-Spatz Disease (HSD) and infantile NAD (INAD) [17]. It is supposed that HSD and INAD are distinct clinical phenotypes of an unique dsorder, despite the different distribution of dystrophic axons (DAs) [8]. In INAD, DAs are ubiquitous in the CNS and they are also found in the peripheral NS (PNS); in HSD they are localized in the globus pallidus and pars reticulata of the substantia nigra.

Here we report the ultrastructural and immunohistochemical comparison of axonal spheroids of two unrelated patients with familial INAD and HSD.

A. Malandrini[1] (✉) · T. Cavallaro · G.M. Fabrizi · G. Berti
Institute of Neurological Sciences, University of Siena, Siena, Italy

Mailing address
[1] A. Malandrini, Istituto di Scienze Neurologiche, Nuovo policlinico, viale Bracci, 2, I-53100 Siena, Italy

Materials and methods

Patients

Case 1

The female patient was the elder daughter of non-consanguineous parents. A sister, now aged 7 years, is affected by a similar disease. The mother and a maternal aunt had strabismus. Psychomotor milestones were delayed. Menarche occurred at 7 years of age. Neurological examination at 9 years of age revealed bilateral convergent strabismus, severe oligophrenia, ataxic gait, marked generalized hypotonia and areflexia, bilateral Babinski vesponses and unintellegible speech. Brain CT scan showed severe cerebellar atrophy. Neurophysiological study indicated neurogenic alterations of the tibialis anterior, biceps brachii and vastus medialis muscles; sensory and motor conduction velocities were normal. Diagnosis of INAD was made on the basis of clinical syndrome and biopsy findings of skin and sural nerve. The patient died at 12 years of age in a neurovegetative state.

Case 2

This female patient was the second born of a non-consanguineous marriage; the elder sister, now aged 19 years, is affected by an identical disease. All psychomotor milestones were delayed. At age 6 years, neurological examination showed axial rigidity, dystonic postures of tongue and extremities, choreoathetotic movements of head and limbs and impaired swallowing and speech. Ophthalmoscopy revealed pigmentary retinopathy. The clinical picture had a severe progressive course and death occurred at 12 years of age after a prolonged, rigid neurovegetative state.

Morphological study

The Brains and spinal cords were fixed for 30 days in 10% neutral formalin. Routine coronal cerebral sections were embedded in paraffin for the following staining: haematoxylin and eosin, Nissl, Woelcke for myelin, Bodian, periodic acid-schiff and Perl's iron reaction.

On selected sections containing a large number of axonal swellings, immunohistochemical analysis was performed using the following antibodies: τ-protein (Sigma, monoclonal, 1:500); 68, 160 and 200 kDa neurofilaments (NFs, Sigma, monoclonal, diluted respectively to 1:30, 1:30 and 1:300); ubiquitin (Dako, polyclonal, 1:100); β-tubulin (Sigma, polyclonal, 1:20); β-amyloid (Boehringer, polyclonal, 1:5); glial fibrillary acidic protein GFAP (Dako, monoclonal, 1:100). Antibody detection was carried out by biotinylated anti-mouse and anti-rabbit antibodies and the vectastain ABC-Elite Kit (Vector) with diaminobenzidine as peroxidase substrate. Sections were counterstained with haematoxylin. We made a comparative study on pallidal DAs from three aged patients dying of cardiac infarction and negative controls included omission of primary antibody.

Biopsy specimens of skin and sural nerve and autopsy samples from representative DA-rich areas of grey and white matter were trimmed into 1–2 mm cubes and processed for electron microscopy (fixed in 2.5% glutaraldehyde postfixed in osmium tetroxide and embedded in Epon resin). Semithin sections were stained with toluidine blue and observed with an Axiomat (Zeiss) light microscope. Ultrathin sections were stained with uranyl acetate and lead citrate and examined with an EM109 (Zeiss) electron microscope.

Results

Light microscopy

Case 1, INAD

Histological examination of sural nerve discloses normal density of myelinated fibres. Axonal enlargements (1–2% of the total axons) with diameter varying from 20 to 50 μm are the most striking feature. Toluidine is unevenly distributed in the axoplasm (Fig. 1A); the myelin sheath is always thin and occasionally absent.

In the skin, bundles of myelinated fibres show similar axonal swellings, but the axoplasm stains more darkly and uniformly with toluidine blue (Fig. 1B). Macroscopic observation of the brain and spinal cord revealed severe atrophy of cerebellum and, to a lesser extgent, of cerebral hemispheres. Histological examination confirms cerebellar cortical atrophy with virtual absence of Purkinje cells; molecular and granular layers are also severely atrophic. Cerebral white matter, corticospinal tracts and posterior columns are diffusely demyelinated with reactive gliosis, confirmed by GFAP immunostaining (data not shown). Axonal swellings are ubiquitous in the cerebellum (Fig. 2), and, to a lesser extent, posterior columns, Goll and Burdach nuclei, cerebral cortex, subcortical cerebral white matter and basal ganglia.

Case 2, HSD

Macroscopic observation revealed rust-brown discoloration of the globus pallidus with remarkable sparing of the pars reticulata of the substantia nigra. Axonal spheroids and iron pigment deposits are selectively localized in the nucleus pallidus (Fig. 3).

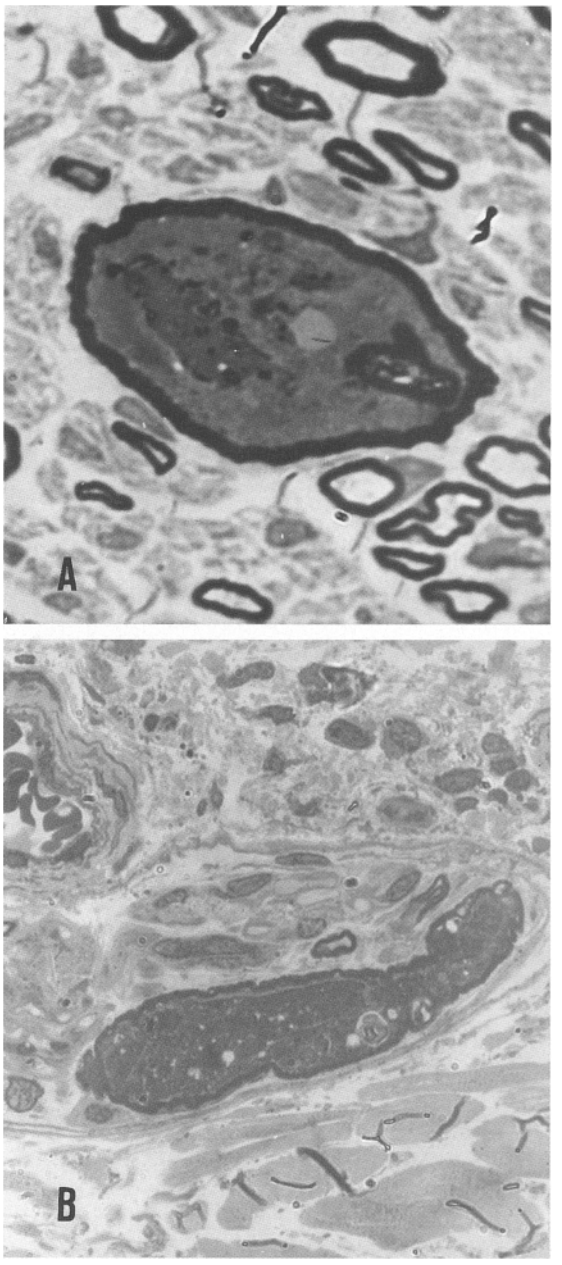

Fig. 1 **A** In the sural nerve we see enormous axonal swelling with thin myelin sheath and non uniformly stained axoplasm. Semithin section, toluidin blue ×600. **B** Cutaneous nerve showing strong homogeneous staining of the enlarged axoplasm (×400)

Electron microscopy

Case 1, INAD

In the sural nerve biopsy DAs are more numerous than suggested by histological observation of myelinated and

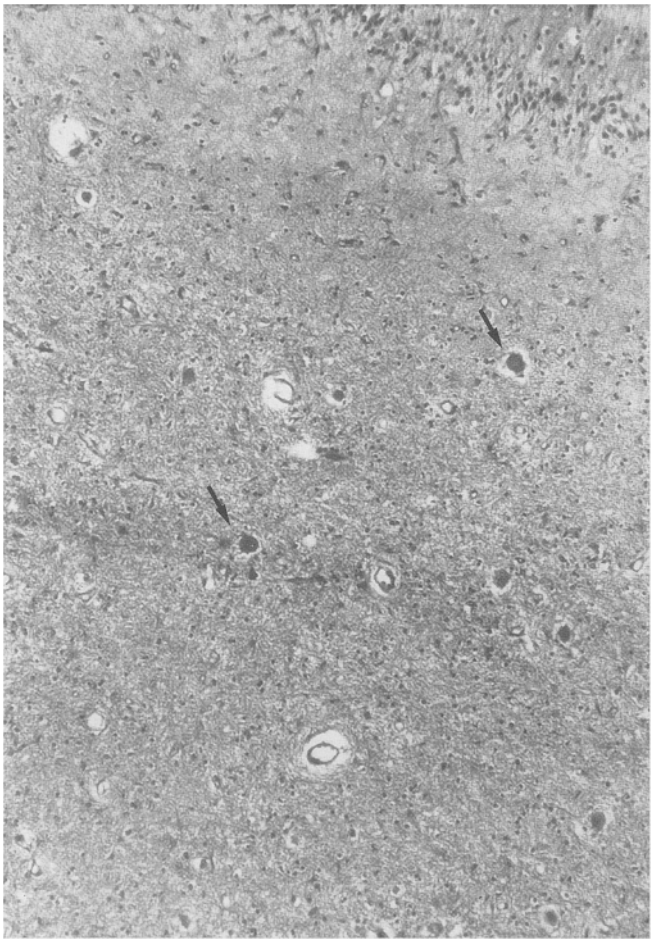

Fig. 2 In the cerebellum axonal spheroids are seen (*arrows*) in the white matter. [Haematoxylin and eosin (H&E) ×100]

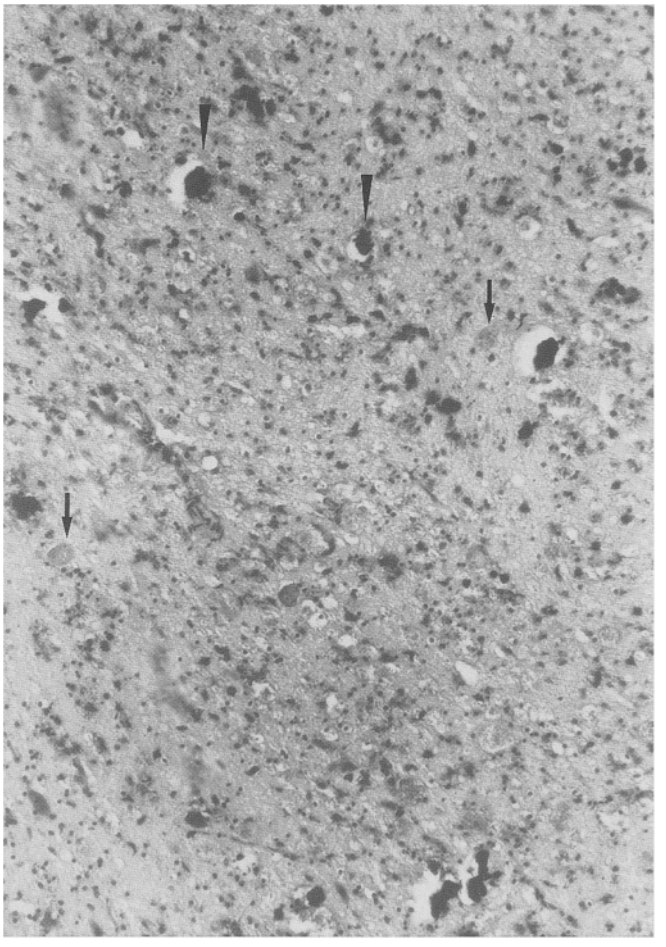

Fig. 3 In the pallidum axonal spheroids (*arrows*) are interspersed among iron deposits (*arrowheads*) (H&E ×120)

unmyelinated fibres. The axons show alterations of graded severity corresponding to the progressive stages of the pathological process. For descriptive utility, we identify three steps of axonal damage. Firstly, DAs with unmodified diameter, containing numerous sparse or tangled branched membrano-utublar profiles and interspersed enlarged, degenerated mitochondria. Neurofilaments are compressed with secondary increased density (Fig. 4A). Secondly, DAs whose axoplasm is composed of sharply demarcated aggregates of tubulo-membranous profiles apparently related to the single unit membrane. Glycogen granules and NFs with rare neurotubules (NTs) are segregated (Fig. 4B, C). In the third step DAs, often without myelin sheath, consist of tightly packed structured material. The enlarged axoplasm is occupied by membrano-tubular profiles, often concentrically arrayed to form paracrystalline structures. Abnormal mitochondria, vesicles, amorphous material and free granules of glycogen are also observed (Fig. 4D). Cutaneous axonal swellings have essentially the same features with an elevated number of packed degenerating mitochondria.

DAs in brain are numerous, ranging in size from 12 to 40 μm; the main axoplasmic component is a granulovesicular membranous material. Occasional aggregates of dense bodies and mitochondria are confined to a corner of the axon (Fig. 5). Few DAs have features resembling the stages 1 and 2 found in the peripheral nerve.

Case 2, HSD

DAs are observed only in the pallidum. They are oval, ranging in size from 20 to 70 μm. The smaller ones are surrounded by a thin myelin sheath and are composed of dense or vesicular bodies, degenerating mitochondria and great amount of amorphous material. The larger ones have no myelin sheath, show an irregular form, and contain predominantly dense or vesicular bodies and enlarged abnormal mitochondria (Fig. 6).

Immunocytochemistry

In both cases axonal swellings are strongly immunoreactive for ubiquitin, while no reaction is detectable for β-amyloid or β-tubulin. Immunoreactivity for τ-protein is stronger in HSD than in INAD (Fig. 7A, B). The immunoreactivity pattern of NF subunits is similar for 68 kDa

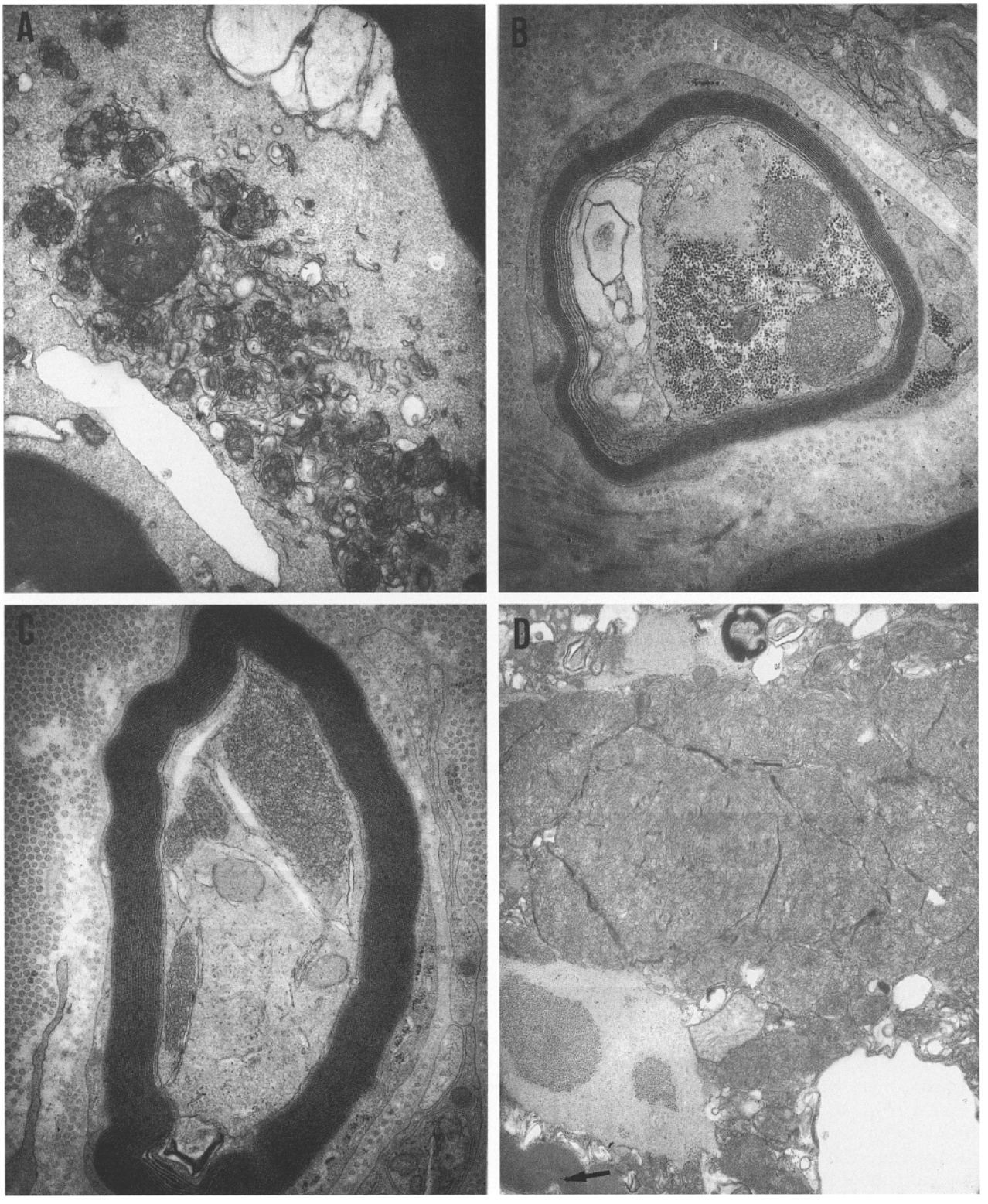

Fig. 4 **A** Transmission electron microscopy of an early-stage axonal spheroid. Proliferation of membranous material in axoplasm with apparently normal cytoskeletal elements (sural nerve, ×15000). **B, C** TEM of an intermediate-stage axonal spheroid. The axoplasm seems organized into compartments with membrano-tubular profiles arraying to form paracrystalline-like aggregates, masses of glycogen and segregation of neurofilaments and rare neurotubules. The membrano-tubular profiles seem to be in relation with the single unit membrane (sural nerve, ×15000). **D** In this TEM the axoplasm is filled with enormous aggreagtes of membrano-tubular elements with small foci of amorphous material and glycogen granules. Note a thin myelin sheath (*arrow*). (Sural nerve, ×16000)

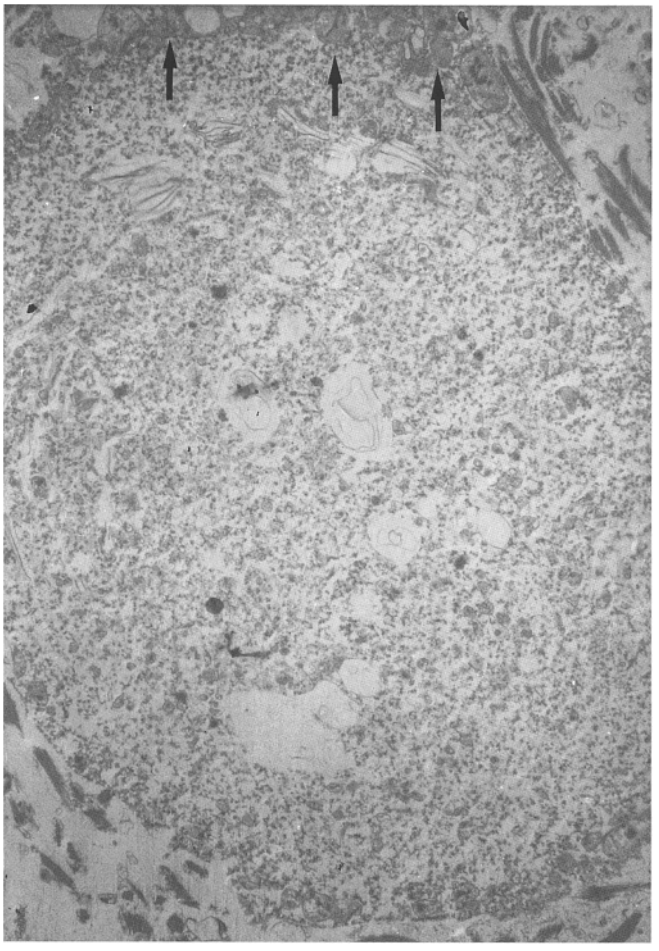

Fig. 5 In the case of infantile neuroxonal dystrophy (INAD) a cerebellar axonal spheroid composed of granulovesicular material is seen; organelles are confined to the edge (*arrow*) (TEM ×8000)

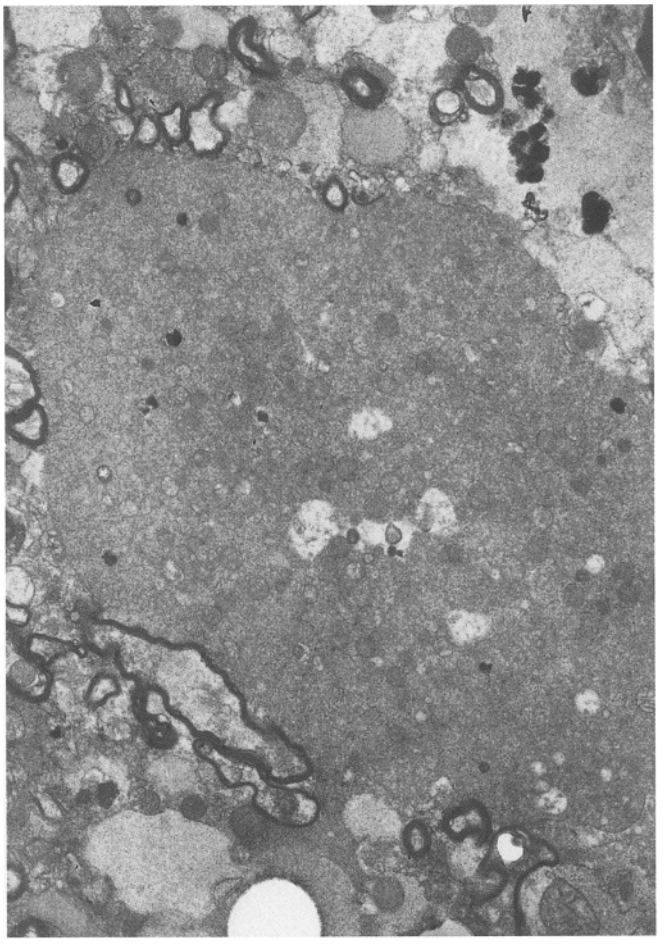

Fig. 6 In the case of Hallervorden-Spatz disease (HSD) we see pallidal axonal spheroids consisting of vesicles, dense bodies and mitochondria in an amorphous matrix. (TEM ×7000)

and 160 kDa, but differs for 200 kDa NF, which is more intense in HSD (Fig. 7D). Staining with all antibodies is granular in HSD and homogeneous in INAD. The immunostaining pattern of large DAs is generally less uniform and intense than that of small ones in both diseases. Normal reactivity to anti-NF antibodies is detected in neurons and axons.

DAs from aged brains show moderate immunoreactivity for ubiquitin, τ-protein, 68 kDa and 160 kDa NF; slight positivity for 200 kDa NF is detected. In all cases the immunostaining patterns is finely granular. No reaction is observed for β-tubulin and β-amyloid.

Discussion

Pathological studies of INAD are numerous and extensive [5, 15, 17], but a detailed ultrastructural and immunohistochemical analysis of HSD-associated DAs is lacking.

In the peripheral nerve and brain of our INAD case, DAs have a similar structure and show a continuum of ultrastructural alterations, varying from mere proliferation of membrano-tubular profiles with unmodified axonal calibre, to large aggregates of membrano-tubular material with no sign of NFs and NTs. These findings suggest progressive evolution of the lesion. The proliferation and/or accumulation of membrano-tubular structures and the consequent progressive loss of cytoskeletal elements seem to be the first morphological events. The membrano-tubular elements may be derived from cisternae of smooth endoplasmic reticulum [8] and may accumulate due to impairment of a step of retrograde axonal transport ("turn-around" mechanism) [3, 60, 20]. Since the membrano-tubular profiles are spatially related to the single unit membrane (Fig. 4B, C), they may alternatively be derived from this structure.

Ultrastructural examination of cerebral DAs in the HSD case reveals a preferential accumulation of dense bodies, degenerating mitochondria and amorphous material, without membrano-tubular profiles and granulo-vesicular material. They do not show any graded and apparently progressive pattern of the pathological alterations.

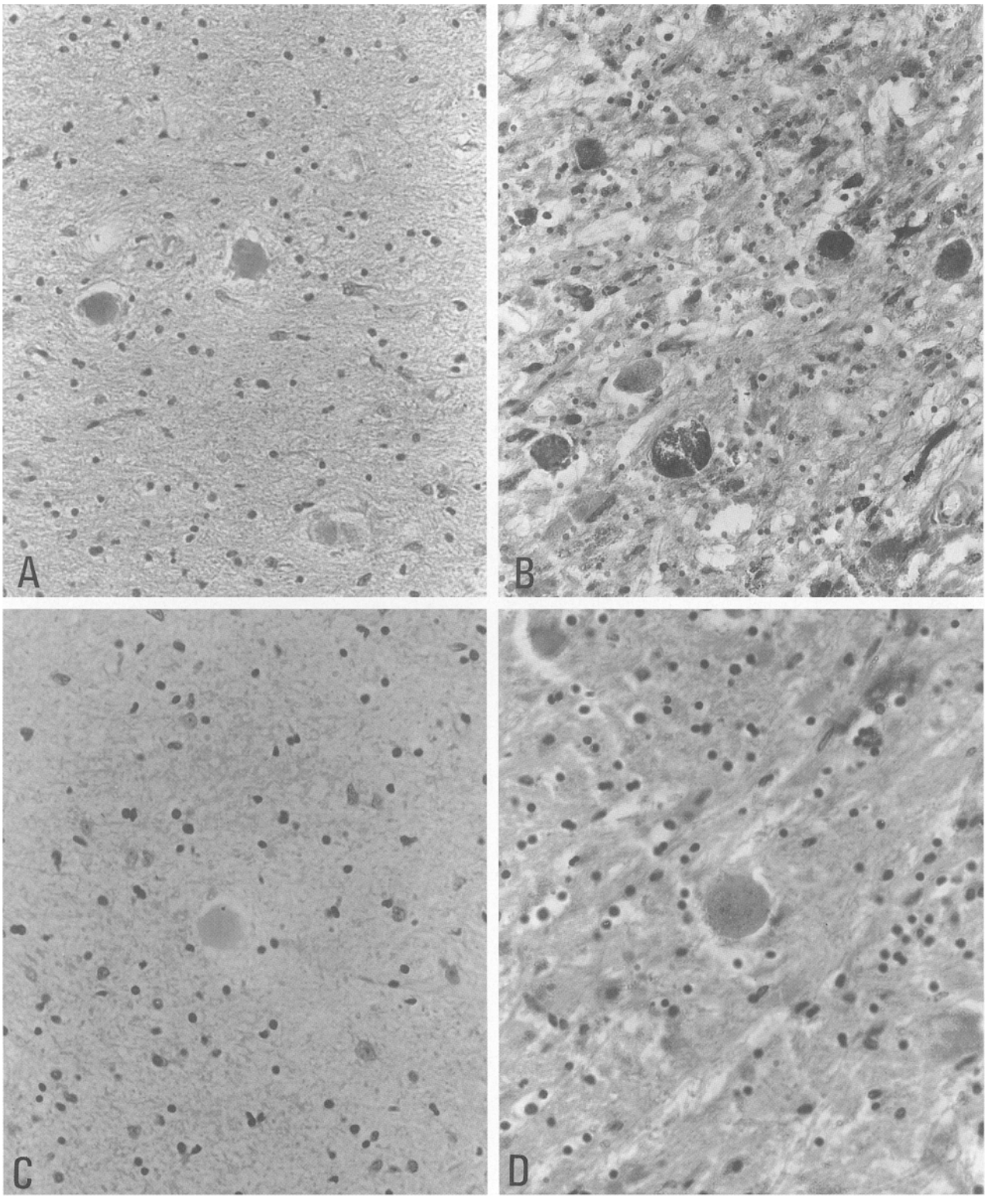

Fig. 7 Immunostaining for τ-protein in INAD (**A**) and HSD (**B**). (×300). Immunostaining for 200 kDa NF in INAD (**C**) and HSD (**D**). (×300). A stronger signal with granular distribution is evident in HSD (**B, D**)

The immunoreactivity for NF subunits in both cases indicates that the accumulated material is partially derived from degraded filamentous proteins which maintain their immunoreactive epitopes in the neutral formalin-treated brain [19]. The more intense staining for the 200 kDa subunit in the HSD-DAs may reflect either a decreased degradation or an overexpression. Overexpres-

sion may be indicated by a higher turnover and dynamic role for the 200 kDa subunit, which plays a crucial role in the assembly of the sister subunits [13, 14, 18]. τ-protein is also more abundant in HSD than in INAD, and has previously been thought to be significant because of its association with Alzheimer paired helical filaments and dystrophic neurites [19]. Since the detection of τ-aggregates in fixed brains is considered to be the consequence of the production of altered forms of τ-protein [10] and since τ-protein seems to the important in determining the axonal shape and cytoskeletal organization, its expression in DAs probably indicates an attempt to repair the axonal damage. Absence of reactivity for β-tubulin is in line with the disappearance of NTs observed at electron microscopy, and also indicates that NFs undergo slower degradation than NTs [4, 20]. The similar pattern of positivity with anti-ubiquitin antibody is consistent with activation of this proteolytic non-lysosomal system in the degradation of damaged or abnormal filamentous cytoskeletal proteins [2, 11, 12]. In the DAs we do not find any expression of β-amyloid, using an antibody against a synthetic peptide. Cochran et al. [3] reported immuno-colocalization of ubiquitin and amyloid-precursor protein (APP) in the DAs from a case of familial INAD. Since APP is a membrane protein that undergoes axonal transport in Alzheimer neuronal cells [9], its presence in DAs could be part of a membrane accumulation, possibly secondary to an alteration of the axonal transport. However, the presence of APP does not necessarily lead to formation and amyloid, as we have shown.

DAs of aged brains show a positive reaction for the same antibodies as HSD and INAD, although with different intensities and patterns of distribution. This similarity is not a surprising finding, and indicates that whatever the pathogenetic mechanism leading to axonal dystrophy, the final result is the accumulation and degradation of cytoskeletal elements, and attempts to remove the accumulated material and repair axonal damage.

Due to the common finding of DAs, it has been proposed that INAD and HSD are phenotypic variants of the same disorder [8, 17]. In our cases, the different ultrastructural appearance and immunoreactivity of DAs suggest a different pathogenetic mechanism. Immunoelectron microscopy and biochemical analysis will help to identify the nature of the accumulated material and to understand the underlying pathogenetic mechanism.

Acknowledgements We thank L. Pannini for skillful technical assistance.

References

1. Aicardi J, Castelein P (1979) Infantile Neuroaxonal Dystrophy. Brain 102:727–748
2. Chiechanover A (1993) The ubiquitin-mediated proteolytic pathway. Brain Pathol 3:67–75
3. Cochran E, Bacci B, Chen Y, Patton A, Gambetti P, Autilio-Gambetti L (1991) Amyloid precursor protein and ubiqutin immunoreactivity in the dystrophic axons is not unique to Alzheimer's disease. Am J Pathol 139 (3):485–489
4. De Leon GA, Mitchell MH (1985) Histological and ultrastructural features of dystrophic isocortical axons in Infantile Neuroaxonal Dystrophy (Seitelberger's Disease). Acta Neuropathol (Berl) 66:89–97
5. Herman MM, Huttenlocher R, Bensch KG (1969) Electron microscopic observations in Infantile Neuroaxonal Dystrophy. Arch Neurol 20:19–33
6. Jakobsen J, Brimijoin S, Sidenius P (1983) Axonal transport in neuropathy. Muscle Nerve 6:164–166
7. Jellinger K (1971) Neuroaxonal dystrophy in man: Character and natural history. Acta Neuropathol (Berl) [Suppl] V:3–17
8. Jellinger K (1973) Neuroaxonal dystrophy: its natural history and related disorders. In: Zimmerman HM (ed) Progress in neuropathology, vol 2. Grune and Stratton Publishers, New York, pp 129–180
9. Koo EH, Sisodia SS, Archer DR, Martin LJ, Weidemann A, Beyreuther K, Fischer P, Masters CL, Price DL (1990) Precursor of amyloid protein in Alzheimer disease undergoes fast anterograde axonal transport. Proc Natl Acad Sci USA 87:1561–1565
10. Kosik KS (1993) The molecular and cellular biology of Tav. Brain Pathol 3:39–43
11. Lowe J, Mayer RJ, Landon M (1993) Ubiquitin in neurodegenerative disease. Brain Pathol 3:66–65
12. Moretto G, Sparaco M, Monaco S, Bonetti B, Rizzuto N (1993) Cytoskeletal changes and ubiquitin expression in dystrophic axons of Seitelberger's disease. Clin Neuropathol 12(1):38–44
13. Nixon RA (1993) The regulation of neurofilament protein dynamics by phosphorylation: clues to neurofibrillary pathology. Brain Pathol 3:29–38
14. Portier MM (1992) Le cytosquelette neuronal: aspects structuraux, fonctionnels et dynamiques. Rev Neurol (Paris) 148(1):1–19
15. Ramackers VT, Lake BD, Harding B, Boyd S, Harden A, Brett EM, Wilson J (1987) Diagnostic difficulties in infantile Neuroaxonal Dystrophy. A clinicopathological study of eight cases. Neuropediatrics 18:170–175
16. Seitelberger F (1952) Eine unbekannte Form von infantiler Lipoid-Speicher-Krankheit des Gehirns. In: Proceedings, First International Congress of neuropathology, Rome, vol 3. Rosenberg and Sellier, Turin, pp 323–333
17. Seitelberger F (1986) Neuroaxonal dystrophy: its relation to aging and neurological diseases. In: Vinken PJ, Bruyn GW, Klawans HL (eds) Handbook of clinical neurology, vol 5. Elsevier Amsterdam, pp 391–415
18. Tokutake S (1990) On the assembly mechanism of neurofilaments. Int J Biochem 22(1):1–6
19. Trojanowski JQ, Schmidt ML, Shin RW, Bramblett GT, Rao D, Lee VM-Y (1993) Altered t- and neurofilament proteins in neurodegenerative diseases: diagnostic implications for Alzheimer's disease and Lewy Body Dementias. Brain Pathol 3:45–54
20. Yoshikawa S, Itoh Y, Nakano T, Oizumi J, Okuyama Y, Aoki K (1985) Diminished retrograde transport causes axonal dystrophy in the nucleus gracilis: electron and light microscopic study. Acta Neuropathol (Berl) 68:93–100